


**Electrocatalysis** Hot Paper

 How to cite: *Angew. Chem. Int. Ed.* **2024**, *63*, e202403674  
 doi.org/10.1002/anie.202403674


# An Electrocatalytic Cascade Reaction for the Synthesis of Ketones Using CO<sub>2</sub> as a CO Surrogate

Ahmed M. Sheta, Sergio Fernández, Changwei Liu, Geyla C. Dubed-Bandomo, and Julio Lloret-Fillol\*

**Abstract:** The construction of carbonyl compounds via carbonylation reactions using safe CO sources remains a long-standing challenge to synthetic chemists. Herein, we propose a catalyst cascade Scheme in which CO<sub>2</sub> is used as a CO surrogate in the carbonylation of benzyl chlorides. Our approach is based on the cooperation between two coexisting catalytic cycles: the CO<sub>2</sub>-to-CO electroreduction cycle promoted by [Fe(TPP)Cl] (TPP = meso-tetraphenylporphyrin) and an electrochemical carbonylation cycle catalyzed by [Ni(bpy)Br<sub>2</sub>] (2,2'-bipyridine). As a proof of concept, this protocol allows for the synthesis of symmetric ketones from good to excellent yields in an undivided cell with non-sacrificial electrodes. The reaction can be directly scaled up to gram-scale and operates effectively at a CO<sub>2</sub> concentration of 10%, demonstrating its robustness. Our mechanistic studies based on cyclic voltammetry, IR spectroelectrochemistry and Density Functional Theory calculations suggest a synergistic effect between the two catalysts. The CO produced from CO<sub>2</sub> reduction is key in the formation of the [Ni(bpy)(CO)<sub>2</sub>], which is proposed as the catalytic intermediate responsible for the C–C bond formation in the carbonylation steps.

Carbonylation reactions are widely used in industry for the synthesis of carbonyl-containing compounds.<sup>[1]</sup> Currently, most carbonylation technologies involve the use of carbon monoxide, usually at high temperature and pressure to drive the carbonylation reactions. The fact that CO is a highly toxic and flammable gas has led researchers to explore other synthetic routes that employ alternative CO sources such as metal carbonyl complexes<sup>[2]</sup> or organic CO surrogates such as ethyl chloroformate,<sup>[3]</sup> DMF,<sup>[4]</sup> and chloroform<sup>[5]</sup> among others. In this line, CO<sub>2</sub> has been identified as a potential CO precursor for carbonylation reaction since it is readily available, inexpensive, and easier to handle.<sup>[6]</sup> However, CO<sub>2</sub> has to be catalytically reduced to CO under thermal hydrogenation conditions or via a two-electron/two-proton transfer process.<sup>[7]</sup> In addition, electrochemistry is a powerful tool to promote carbonylation reactions.<sup>[8]</sup> In this regard, a promising approach is the formation of CO from the electrocatalytic CO<sub>2</sub> reduction reaction (CO<sub>2</sub>RR). Several molecular complexes and materials based on transition metals have been reported as highly active and selective electrocatalysts for CO<sub>2</sub> reduction to CO.<sup>[9]</sup> Among molecular electrocatalysts, iron porphyrins are some of the most active and selective molecular electrocatalysts for the CO<sub>2</sub> reduction to CO in organic solvents, as shown by Savéant and co-workers.<sup>[10]</sup>

Despite the potential benefits of using CO<sub>2</sub> as a CO surrogate in carbonylation reactions, few methods have been successfully employed due to their inherent reactivity in delivering carboxylation products under electrochemical conditions.<sup>[11]</sup> To overcome these challenges, Périchon and co-workers developed a pioneering stepwise electrochemical/chemical method for the stoichiometric synthesis of ketones using CO<sub>2</sub> (Scheme 1).<sup>[12]</sup> In this work, the active [Ni(bpy)(CO)<sub>2</sub>] species was formed in situ at the cathode through electrolysis of [Ni(bpy)(Br)<sub>2</sub>] (**1Ni**) in the presence of CO<sub>2</sub> (Scheme 1, top). In a subsequent step, the redox potential was switched off, the atmosphere was replaced by argon, and the substrate was added to the [Ni(bpy)(CO)<sub>2</sub>] solution giving the corresponding symmetric ketone stoichiometrically. Catalytic versions of this reaction were achieved by using CO gas<sup>[13]</sup> and metal-carbonyl precursors<sup>[14]</sup> as CO sources. More recently, Skrydstrup, Daasbjerg and co-workers developed a set of classical Pd-catalyzed carbonylation reactions using employing the CO generated from CO<sub>2</sub>RR in a separated compartment where an iron porphyrin [Fe(TPP)Cl] was used as electrocatalyst in DMF electrolyte solution (Scheme 1, middle).<sup>[15]</sup> The idea of

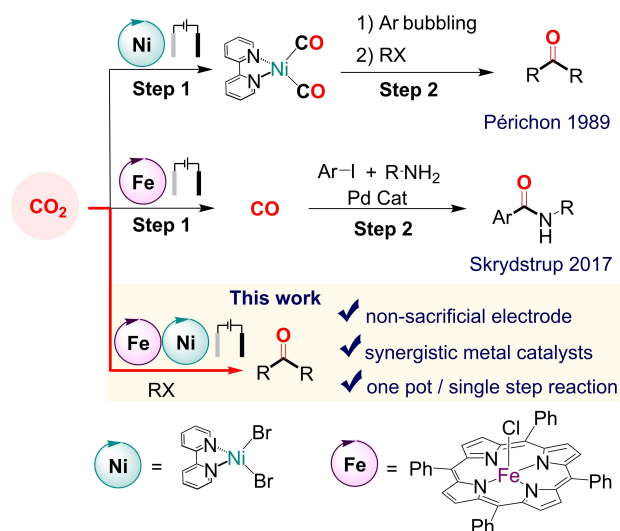
[\*] A. M. Sheta, Dr. S. Fernández, C. Liu, Dr. G. C. Dubed-Bandomo, Prof. Dr. J. Lloret-Fillol  
 Institute of Chemical Research of Catalonia (ICIQ), Barcelona Institute of Science and Technology, Avda. Països Catalans, 16, 43007 Tarragona (Spain)  
 E-mail: jlloret@iciq.es

A. M. Sheta, C. Liu  
 Departament de Química Orgànica i Analítica, Universitat Rovira i Virgili, Carrer Marcel·lí Domingo s/n, 43007 Tarragona (Spain)

A. M. Sheta  
 Department of Chemistry, Damietta University, Damietta El-Gadeeda City, Kafr Saad, Damietta Governorate, 34511 (Egypt)

Prof. Dr. J. Lloret-Fillol  
 Institution for Research and Advanced Studies (ICREA), Passeig Lluís Companys, 23, 08010 Barcelona (Spain)

© 2024 The Authors. Angewandte Chemie International Edition published by Wiley-VCH GmbH. This is an open access article under the terms of the Creative Commons Attribution Non-Commercial NoDerivs License, which permits use and distribution in any medium, provided the original work is properly cited, the use is non-commercial and no modifications or adaptations are made.



**Scheme 1.** Electrochemical approaches to use  $\text{CO}_2$  as a carbonyl source.

producing CO from  $\text{CO}_2$  electroreduction in a separate chamber where it will be used was further explored at ambient pressure<sup>[16]</sup> but also at challenging high pressure. In this regard, two seminal contributions are highlighted.<sup>[17]</sup> T. Cantat, M. Fontecave and co-workers reduced  $\text{CO}_2$ -to-CO in a high-pressure electrolytic cell containing a bimetallic ZnAg catalyst at the cathode, where the propylene oxide was carbonylated by thermal catalysis at high-pressure  $\text{CO}$ .<sup>[17a]</sup> Additionally, Miller, Liu, Wang and co-workers have reported the Pd-catalyzed synthesis of polyketones through ethylene carbonylation using a multicompartiment high-pressure electrochemical reactor.<sup>[17b]</sup> In that case, a Pd cathode was used as a  $\text{CO}_2$ -to-CO reduction electrocatalyst.

To our knowledge, a single-compartment fully electrochemical cascade scheme where the  $\text{CO}_2$ -to-CO reduction catalytic cycle is coupled to electrocatalytic organometallic carbonylation is still missing in the literature. While this approach has the potential to offer several benefits, such as simple experimental setups and straightforward synthetic protocols, it is also very challenging due to the need to match the kinetics of two or more electrocatalytic cycles in a single compartment, which remains a challenge in the electrocatalysis and electrosynthesis community.<sup>[18]</sup>

As a proof of concept, we herein explore the direct use of  $\text{CO}_2$  as a CO surrogate in the carbonylation of benzyl chlorides through the synergistic combination of two different earth-abundant metal electrocatalysts: the well-established  $\text{CO}_2$  reduction electrocatalyst *meso*-tetraphenylporphyrin iron(III) chloride (**FeTPPCl**) and  $[\text{Ni}(\text{bpy})\text{Br}_2]$  (**1Ni**) as a potential carbonylation pre-catalyst. This method allows synthesizing symmetric ketones from good to excellent yields in one pot, in an undivided cell and with non-sacrificial electrodes. However, the use of a sacrificial electron donor is necessary. The reaction operates through an electrochemical cascade mechanism in which the  $\text{CO}_2$  reduction and carbonylation electrocatalytic cycles operate

synergistically, as the observed reactivity and mechanistic studies suggested.

We selected benzyl chloride (**1a**) as our model substrate to initiate the investigation. After a pre-screening of reaction conditions (Supporting Information section 3), using **FeTPPCl** (2 mol%) to in situ generate CO from  $\text{CO}_2$  electroreduction, **1Ni** (5 mol%) as the carbonylation catalyst, and Fe/Ni (alloy-64/36) sacrificial anode (Table 1, Entry 2) the symmetric ketone **2a** was obtained in 49% yield. In addition, phenylacetic acid (**4a**), dibenzyl (**3a**) and toluene (**5a**) were also obtained. Replacement of the sacrificial anode with a carbon electrode produced **2a** in equivalent yield. However, adding triethylamine (TEA) as an electron and proton source led to the full conversion of benzyl chloride and yielding 90% of **2a** (Table 1, Entries 1–3, and Supporting Information Table S2).

Blank experiments showed that ketone **2a** was not formed when the reaction was carried out without redox potential or **1Ni**. However, in the absence of **1Ni**, toluene (**5a**) and phenylacetic acid (**4a**) were obtained (Table 1, Entry 4). The minimum amount of **1Ni** to obtain a virtual quantitative carbonylation yield was 5 mol%. Less than 5 mol% of **1Ni** increased the carboxylation and toluene products (Table 1, Entry 5). On the other hand, increasing the amount of **1Ni** up to 10% yields 90% of the ketone (Table 1, Entry 6). Interestingly, in the absence of **FeTPPCl** the ketone yield was low (16% yield), regardless that the **1Ni** percentage was increased (yielding **2a** in 27% at 15%

**Table 1:** Optimization of the carbonylation of benzyl chloride.<sup>[a]</sup>

| Entry | Deviation from the standard conditions        | Yield (%) <sup>[b]</sup> |    |    |    | Conv (%) |
|-------|---|--------------------------|----|----|----|----------|
|       |   | 2a                       | 3a | 4a | 5a |          |
| 1     | Standard conditions maintained <sup>[a]</sup> | 90 <sup>[c]</sup>        | 0  | 4  | 1  | 98       |
| 2     | Fe/Ni anode, <sup>[d]</sup> no TEA            | 49                       | 12 | 12 | 21 | 100      |
| 3     | no TEA  | 47                       | 0  | 26 | 18 | 87       |
| 4     | no <b>1Ni</b>                                 | 0                        | 0  | 40 | 49 | 92       |
| 5     | <b>1Ni</b> (2 mol%)                           | 33                       | 7  | 36 | 20 | 98       |
| 6     | <b>1Ni</b> (10 mol%)                          | 90                       | 1  | 1  | 6  | 100      |
| 7     | no <b>FeTPPCl</b>                             | 16                       | 1  | 15 | 60 | 95       |
| 8     | no <b>FeTPPCl</b> , <b>1Ni</b> (15 mol%)      | 27                       | 2  | 14 | 40 | 85       |
| 9     | no <b>FeTPPCl</b> & no <b>1Ni</b>             | 0                        | 6  | 20 | 60 | 90       |
| 10    | <b>FeTPPCl</b> (1 mol%)                       | 78                       | 0  | 5  | 10 | 95       |
| 11    | <b>FeTPPCl</b> (3 mol%)                       | 73                       | 0  | 1  | 21 | 98       |
| 12    | $\text{CO}$ atm., no <b>FeTPPCl</b>           | 69                       | 1  | 0  | 22 | 94       |

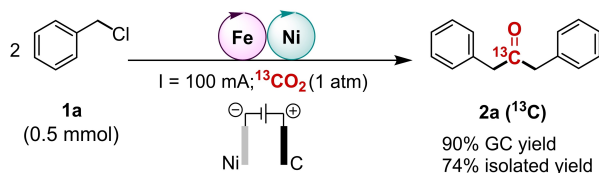
[a] Standard conditions: **1a** (63 mg, 0.5 mmol),  $\text{CO}_2$  (1 atm), nickel foam as cathode, graphitic carbon as anode,  $[\text{TBA}]\text{BF}_4$  (0.03 M), TEA (2.0 eq.), DMF (5 mL), **1Ni** (5 mol%), **FeTPPCl** (2 mol%), single compartment cell, current of 100 mA during 3 h at room temperature. Electrasyn 2.0 or power supply (see the Supporting Information). [b] Yield and conversion determined by GC and  $^1\text{H}$  NMR analysis as two experiments average. [c] 86% isolated yield of **2a**. [d] Fe/Ni (64/36).

**1Ni**, Table 1, Entry 7&8). Although this suggests that **1Ni** can catalyze the CO<sub>2</sub> reduction to CO and carbonylation reactions, the selectivity is an issue when **1Ni** is the only catalyst. In this circumstance, the carbonylation reaction (27%) has as parallel reaction catalytic processes that does not use CO, like the carboxylation (14%) and dehalogenation (40%) reactions. In concordance, replacing the CO<sub>2</sub> atmosphere with CO yields **2a** but in a lower yield (69%) (Table 1, Entry 12). Nevertheless, the best performances were obtained with the dual catalytic system **1Ni** / **FeTPPCL**. However, the **FeTPPCL** percentage should be properly adjusted. As expected, a lower **FeTPPCL** percentage than the optimal was detrimental to the yield. A higher **FeTPPCL** percentage was also detrimental, suggesting that the **FeTPPCL** is not solely electroreducing the CO<sub>2</sub>-to-CO (Table 1, Entry 9, 10 and 11) but the low valent iron porphyrin formed can react with BnCl as previously observed (See further discussion below).<sup>[19]</sup>

When the reaction was performed without a CO<sub>2</sub> atmosphere, a 3% of **2a** was obtained. Although minor, one could speculate that DMF could be a CO surrogate. However, the experiment replacing DMF with acetonitrile as a solvent under CO<sub>2</sub> produced the ketone in a good yield, but **2a** was not detected if the reaction was conducted under Ar (Table S5), reinforcing the role of CO<sub>2</sub> as CO surrogate. Moreover, the carbonyl source in **2a** was confirmed through <sup>13</sup>C labelling studies of benzyl chloride employing <sup>13</sup>CO<sub>2</sub>, which resulted in the formation of **2a** (<sup>13</sup>C) (Scheme 2). These experiments agree with CO<sub>2</sub> as the origin of the CO in the formed ketone.

Then, we evaluated the generality of the CO<sub>2</sub>-to-CO reduction catalyst. We tested other well-known catalysts such as Cobalt(II) phthalocyanine (**CoPc**), (*fac*-Mn(**bpy**)-(CO)<sub>3</sub>Br), ([Ni(**cyclam**)](PF<sub>6</sub>)<sub>2</sub>) and silver nanoparticles (**Ag-NP**). Using our standard conditions, **CoPc**, **Ag-NP** and [Ni(**cyclam**)](PF<sub>6</sub>)<sub>2</sub> gave only a moderate ketone yield, while no ketone was detected with *fac*-Mn(**bpy**)-(CO)<sub>3</sub>Br (Table 2).

With the optimized conditions in hand, we examined the reaction scope of benzyl chloride derivatives, obtaining from moderate to high yield of the carbonylated products. Substrates containing electron-donating groups gave a high yield of the ketones (Table 3, compounds **2a**, **2b**, **2c**, **2d**, **2e** & **2h**), while substrates containing electron-withdrawing groups gave moderate or low yield (Table 3, compounds **2f**, **2g**, **2i** & **2j**). Substrates with methoxy groups showed anodic



**Scheme 2.** <sup>13</sup>C labelling. Standard conditions: **1a** (63 mg, 0.5 mmol), <sup>13</sup>CO<sub>2</sub> (1 atm), nickel foam as cathode, graphitic carbon as anode, [TBA]BF<sub>4</sub> (0.03 M), TEA (2.0 eq.), DMF (5 mL), **1Ni** (5 mol%), **FeTPPCL** (2 mol%), single compartment cell, current of 100 mA during 3 h at room temperature. Electrasyn 2.0.

**Table 2:** CO<sub>2</sub> reduction catalyst scope.<sup>[a]</sup>

| Entry | CO <sub>2</sub> R Catalyst                           | Yield (%) <sup>[b]</sup> |           |           |           | Conv. (%) |
|-------|--|--------------------------|-----------|-----------|-----------|-----------|
|       |  | <b>2a</b>                | <b>3a</b> | <b>4a</b> | <b>5a</b> |           |
| 1     | None   | 16                       | 1         | 15        | 60        | 95        |
| 2     | <b>FeTPPCL</b>                                       | 90                       | 0         | 4         | 1         | 98        |
| 3     | <b>CoPc</b>  | 36                       | 3         | 9         | 40        | 95        |
| 4     | <b>Ag-NP</b>   | 28                       | 0         | 21        | 39        | 90        |
| 5     | [Ni( <b>cyclam</b> )](PF <sub>6</sub> ) <sub>2</sub> | 26                       | 0         | 16        | 39        | 92        |
| 6     | <i>fac</i> -Mn( <b>bpy</b> )-(CO) <sub>3</sub> Br    | 0                        | 0         | 36        | 48        | 90        |

[a] Standard conditions: **1a-j** (63 mg, 0.5 mmol), CO<sub>2</sub> (1 atm), nickel foam as cathode, graphitic carbon as anode, [TBA]BF<sub>4</sub> (0.03 M), TEA (2.0 eq.), DMF (5 mL), **1Ni** (5 mol%), CO<sub>2</sub>R catalyst (2 mol%), single compartment cell, current of 100 mA during 3 h at room temperature. Electrasyn 2.0 [b] Yield and conversion determined by GC and <sup>1</sup>H NMR analysis as two experiments average.

**Table 3:** Evaluated substrates for the electro-carbonylation reaction.<sup>[a,b]</sup>

| Substrate        | Yield (%) |
|------------------|-----------|
| <b>2a</b>        | 86%       |
| <b>2b</b>        | 84%       |
| <b>2c</b>        | 81%       |
| <b>2d</b> (para) | 82%       |
| <b>2e</b> (meta) | 59%       |
| <b>2f</b>        | 62%       |
| <b>2g</b>        | 44%       |
| <b>2h</b>        | 72%       |
| <b>2i</b>        | 53%       |
| <b>2j</b>        | <5%       |

[a] General conditions: **1a-j** (63 mg, 0.5 mmol), CO<sub>2</sub> (1 atm), nickel foam as cathode, graphitic carbon as anode, [TBA]BF<sub>4</sub> (0.03 M), TEA (2.0 eq.), DMF (5 mL), **1Ni** (5 mol%), **FeTPPCL** (2 mol%), single compartment cell, current of 100 mA during 3 h at room temperature. Electrasyn 2.0 or power supply (see the Supporting Information).<sup>[b]</sup> yield in the table is the isolated yield. <sup>[c]</sup> 10 eq of TEA were used for those substrates.

oxidation yielding the corresponding aldehydes and alcohols, and this problem was solved by increasing the sacrificial electron donor (10 eq. of TEA).

In addition, the reaction was scaled up to gram scale by employing a larger cell (4-fold higher electrode surface) and implemented a recirculation system from a reservoir. This setup enabled us to transform 150 mL from a reservoir containing 15 mmol of BnCl to produce 1.1 g of the ketone

(70 %), demonstrating the scalability of our method (See Supporting Information, Figure S1).

To explore the ability of our electrochemical cascade to lower CO<sub>2</sub> concentrations, we investigated the potential for ketone formation at CO<sub>2</sub> concentrations of 10 %, yielding an impressive 88 % of ketone, marginally lower than the 90 % yield achieved with 100 % CO<sub>2</sub> concentration. This result underscores the robustness of our methodology with diluted CO<sub>2</sub> sources, which could facilitate exploiting low concentration CO<sub>2</sub> sources (Table S7).

Benzyl chlorides performed significantly better than bromides, which can be rationalized based on previous studies suggesting that benzyl radicals can be produced directly by the electrode yielding homocoupling products.<sup>[20]</sup> We also found that aliphatic substrates did not form ketones. On the other hand, attempts to synthesize asymmetric ketones underscore the necessity for matched reaction kinetics of both substrates to facilitate carbonylation avoiding the formation of the cross-coupling product (Supporting Information Tables S9a–S9f).

To shed light on the reaction mechanism, we first studied the evolution of the reaction. Interestingly, we observed that the BnCl consumption and ketone formation were decoupled from the CO detection for the first 30 min of the reaction. We rationalize that the CO formed is directly involved in the carbonylation reaction (Figure 1) and only accumulates after the reaction rate slows down due to decreased substrate concentration.

Then, we conducted cyclic voltammetry (CV) for both catalysts under Ar and CO<sub>2</sub>, in the presence and absence of BnCl (Figure 2). The CV of **Fe<sup>II</sup>TPPCI** under Ar (Figure 2, top) shows the single reduction events of Fe<sup>III/II</sup>, Fe<sup>II/I</sup> and formal Fe<sup>I/0</sup> at –0.7, –1.5 V and –2.1 V vs. Fc<sup>+/0</sup>, respectively. Under CO<sub>2</sub>, it is observed the well-known catalytic CO<sub>2</sub> reduction at the formal Fe<sup>I/0</sup> redox wave, as previously reported.<sup>[21]</sup> Under Ar, it can also be observed the reported reaction of Fe<sup>I/0</sup> redox wave with BnCl (1 eq), which has been ascribed to the formation of **Fe<sup>II</sup>TPP-alkyl** intermedi-

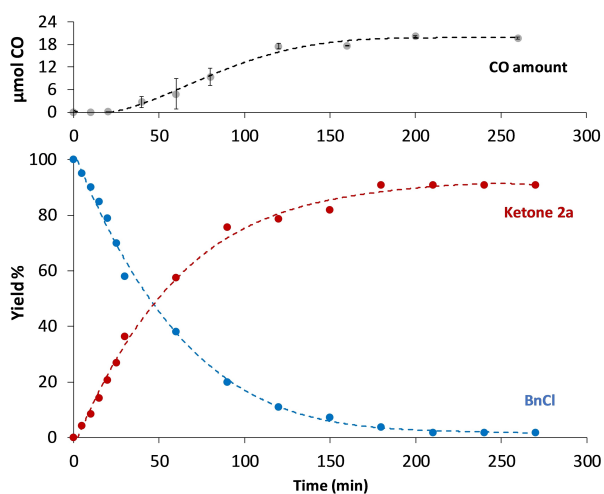


**Figure 1.** Electrochemical reduction of CO<sub>2</sub> and carbonylation of benzyl chloride. The yield of CO, ketone **2a** and consumption of the substrate.

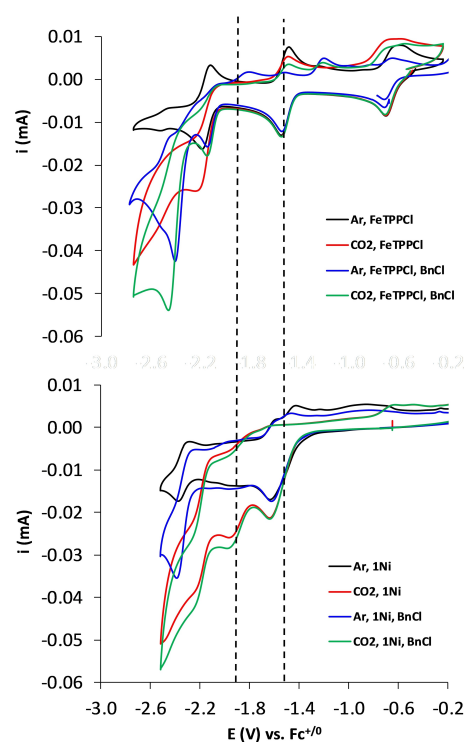


**Figure 2.** CVs of **Fe<sup>II</sup>TPPCI** (1 mM) and **1Ni** (1 mM) in anhydrous TBABF<sub>4</sub>/DMF (0.1 M) solution at 0.1 = vV · s<sup>-1</sup>, glassy carbon WE (Ø = 0.3 cm), Ag pseudo-RE (Ag wire in TBABF<sub>4</sub>-DMF 0.1 M) and Pt wire CE. Under Ar (black) and with added BnCl (1 eq) under Ar (blue) and CO<sub>2</sub> (red) with added BnCl (1 eq) under CO<sub>2</sub> (green).

ate via S<sub>N</sub><sup>2</sup> reaction.<sup>[19,22]</sup> The formation of organometallic **Fe<sup>II</sup>TPP-Bn** species has also recently been proposed as key by Macmillan and coauthors in the photocatalyzed S<sub>H</sub><sup>2</sup> reactions.<sup>[23]</sup> Further electrochemical reduction triggers a catalytic wave at –2.2 V vs. Fc<sup>+/0</sup>.<sup>[24]</sup>

The catalytic wave can be explained by a sequence of events starting with a single electron reduction of the (**Fe<sup>II</sup>TPP-Bn**) to yield (**Fe<sup>I</sup>TPP-Bn**), which is followed by either i) a dissociation process that forms a benzyl radical and Fe<sup>0</sup>, re-engaging in the BnCl activation. Then, the benzyl radical should be reduced by the electrode. ii) A metal-carbon heterolytic bond cleavage, forming the benzyl anion and formal **Fe<sup>I</sup>TPP**. One electron reduction of **Fe<sup>I</sup>TPP** recovers the formal **Fe<sup>0</sup>TPP**, the initial species that reacts with BnCl. Based on the literature, we presume the main mechanism goes through (ii).<sup>[25]</sup>

Interestingly, in the presence of CO<sub>2</sub> and BnCl, the Fe<sup>I/0</sup> redox wave resembles the one observed under Ar, but with slightly higher intensity. The same occurs for the subsequent catalytic wave. Previous studies indicate that the CO and CO<sub>2</sub> insertion in the iron carbon bond of **Fe<sup>II</sup>TPP-Bn** species is unlikely.<sup>[22d,26]</sup> Therefore, the role of the **Fe<sup>II</sup>TPPCI** could potentially be dual; the CO<sub>2</sub> reduction to CO and the BnCl activation via the **Fe<sup>II</sup>TPP-Bn** species catalyzing the formation of benzyl anion.

CV of **1Ni** under Ar (Figure 2, bottom) represents a complex redox event at –1.6 V vs Fc<sup>+/0</sup>, which was previously attributed to the reduction of Ni<sup>II</sup> to Ni<sup>I</sup>, followed

by a disproportionation process ( $\text{Ni}^{\text{I}}$  to yield  $\text{Ni}^0$  and  $\text{Ni}^{\text{II}}$ ) which is common for many of the catalytic cycles proposed for **1Ni**.<sup>[27]</sup> The redox event at lower redox potential ( $-2.4$  V vs  $\text{Fc}^{+/0}$ ) corresponds to the reduction of the remaining  $\text{Ni}^{\text{I}}$  to  $\text{Ni}^0$ . Under  $\text{CO}_2$ ,  $[\text{Ni}(\text{bpy})(\text{CO})_2]$  is formed as previously proposed.<sup>[12]</sup> Then, the addition of  $\text{BnCl}$  does not greatly affect the CV, particularly under  $\text{CO}_2$ , and the intensity of the event is much lower in comparison to **FeTPPCI**, which increases dramatically (See SI, Figure S3&S4).

We then studied the reaction of the  $[\text{Ni}(\text{bpy})\text{Br}_2]$  with  $\text{CO}_2$  by IR spectroelectrochemistry (IR-SEC, Figure 3), following previous studies but under our catalytic reaction conditions.<sup>[28]</sup> Several IR bands appeared during the first reduction process at the  $\text{Ni}^{\text{II/I}}$  wave ( $-1.2$  V). The most prominent peaks at  $1974$  and  $1897$   $\text{cm}^{-1}$ , increased together as a function of potential, suggesting that they belong to the same species. The same two peaks were observed during the experiment under  $\text{CO}$  atmosphere (Figure S7), suggesting Ni-carbonyl species' formation. These IR features are consistent with the formation of  $[\text{Ni}(\text{bpy})(\text{CO})_2]$ , and matched previously reported data from the isolated  $[\text{Ni}(\text{bpy})(\text{CO})_2]$  in the solid state.<sup>[29]</sup> Significant changes occur upon sweeping the applied potential to  $-2.0$  V. While the peaks assigned to  $[\text{Ni}(\text{bpy})(\text{CO})_2]$  decrease, new broad signals appear at lower energies (ca.  $1960$ ), in line with the

formation of further reduced Ni-CO species. For instance, the DFT calculated IR spectrum of the reduced  $[\text{Ni}(\text{bpy})(\text{CO})_2]^-$  shows two vibrations at  $1955$   $\text{cm}^{-1}$  and  $1868$   $\text{cm}^{-1}$ . The new broad band at  $2040$   $\text{cm}^{-1}$  is assigned to  $[\text{Ni}(\text{CO})_4]$ .<sup>[30]</sup> Therefore, the high  $\text{CO}$  concentration built up close to the electrode surface at too negative potentials leads to the bpy ligand dissociation. Nonetheless, electrochemical experiments starting from **1a** and a  $\text{Ni}^0$  source such as  $[\text{Ni}(\text{COD})_2]$  under a  $\text{CO}$  atmosphere did not yield the corresponding carbonylation product (**2a**). Instead, toluene was observed, suggesting that  $[\text{Ni}(\text{CO})_4]$  is not an active intermediate in the carbonylation process.

Then, the presence of  $\text{BnCl}$  significantly changes the speciation in the SEC experiment (Figure 3). Besides the formation of  $[\text{Ni}(\text{bpy})(\text{CO})_2]$ , new shoulders at  $1870$   $\text{cm}^{-1}$  appears (blue curve), which intensify at more reducing redox potentials (red curve). These new intense peaks could correspond to carbonyl vibrations of the nickel alkyl intermediate after the activation of the  $\text{BnCl}$  by the  $[\text{Ni}(\text{bpy})(\text{CO})_2]$ . At the same time, the presence of  $\text{BnCl}$  avoids the formation of the previous peaks assigned to  $[\text{Ni}(\text{CO})_4]$ .

IR-SEC experiments in the presence of **FeTPPCI** also provide valuable information. One main difference observed between the SEC with **1Ni** alone and **1Ni**+**FeTPPCI** is the clearer formation of  $2040$   $\text{cm}^{-1}$  and  $1960$   $\text{cm}^{-1}$  peaks. While the former can be attributed to  $[\text{Ni}(\text{CO})_4]$ , the latter is a new speciation. Interestingly, the peak at  $1960$   $\text{cm}^{-1}$  is more pronounced in the presence of  $\text{BnCl}$ . This observation suggests that this peak ( $1960$   $\text{cm}^{-1}$ ) could be attributed to a new nickel species related to the higher concentration of  $\text{CO}$  and resulting products from the activation of  $\text{BnCl}$ , as no significant peak was observed when the SEC was performed without the **1Ni**. By studying the IR spectra of potential speciation by DFT calculations, the peak at  $1960$   $\text{cm}^{-1}$  could be attributed to  $[\text{Ni}(\text{bpy})(\text{Bn})_2(\text{CO})]$ .

Considering the data, we highlight the following aspects that help to simplify and rationalize the role of the two catalysts. Both **FeTPPCI** and **1Ni** are necessary to obtain the ketone in good yield, but **1Ni** alone can yield the ketone albeit in lower yield (16–27%), while the **FeTPPCI** alone cannot (only toluene and carboxylation products are obtained, no-homo-dimer formation). **FeTPPCI** can catalyze the reduction of  $\text{CO}_2$ -to- $\text{CO}$  and  $\text{BnCl}$ -to- $\text{Bn}^-$  anion.  $\text{Bn}^-$  anion protonation yielding toluene covers the observed better yields of the ketone when anhydrous media is used in the standard catalytic conditions. Since no ketone is observed with **FeTPPCI** alone the carbonylation should occur at the nickel coordination sphere but also that a portion of the  $\text{BnCl}$  activated could also be derived from the **FeTPPCI** activity. Therefore, the mechanism is more complex and a second role for the catalysts should be contemplated. Nevertheless, at the first level, one can simplify this complexity into a scenario where the **FeTPPCI** catalyst's main role is the  $\text{CO}_2$ -to- $\text{CO}$  electroreduction, and the **1Ni** role is to activate the  $\text{BnCl}$  and form the C–C bond formation and carbonylation. However, based on the experimental data, it cannot be neglected that **1Ni** can also reduce  $\text{CO}_2$ -to- $\text{CO}$ , although inefficiently, and the  $\text{Bn}^-$  anion could be catalytically formed by the **FeTPPCI**, introducing

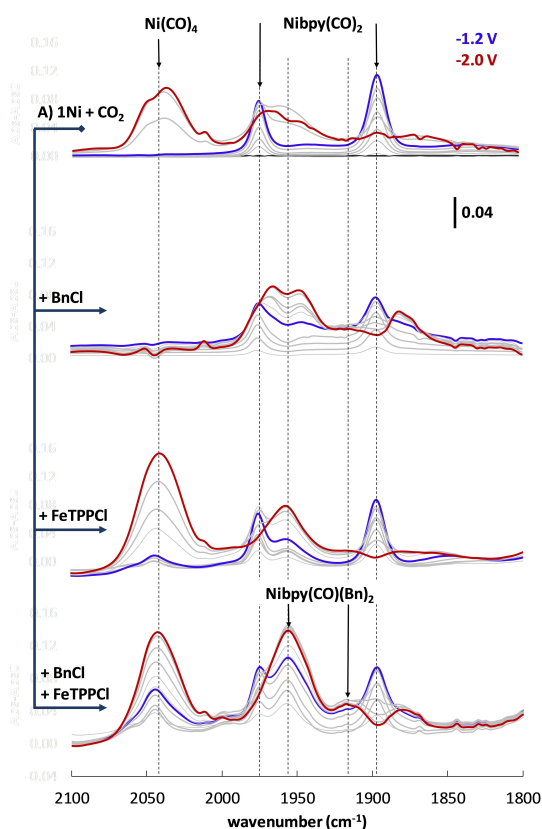


**Figure 3.** IR-SEC of  $[\text{Ni}(\text{bpy})\text{Br}_2]$  (**1Ni**) (6 mM) in  $\text{DMF}/\text{TBAPF}_6$  (0.2 M) under  $\text{CO}_2$  atmosphere (A). The graphs represent the differential spectra in  $\text{Abs}-\text{Abs}_0$  versus wavenumber ( $\text{cm}^{-1}$ ). OTTE cell Pt (WE), Pt (CE), Ag (RE). From top to bottom A) +  $\text{BnCl}$  (60 mM), A) + **FeTPPCI** (2.4 mM) and A) +  $\text{BnCl}$  (60 mM), + **FeTPPCI** (2.4 mM).

an unanticipated synergy between both catalysts. In line with the proposed synergistic reactivity between both metal complexes (**1Ni** and **FeTTPCI**) an increase in redox potential not only boosts the reaction yield but also enhances the selectivity. At redox potentials where only the **1Ni** is reduced, the ketone selectivity is modest. However, at more reducing potentials, where **1Ni** and **FeTTPCI** are reduced, we observed significant increase in both yield and the selectivity (Figure S7 and table S8). Considering all the data collected, we proposed the mechanism depicted in Scheme 3 as a hypothesis to rationalize the catalytic activity observed.

In summary, we demonstrated that CO<sub>2</sub> can be used as a CO surrogate in the carbonylation of benzyl chlorides, utilizing a combination of two earth-abundant metal catalysts in an undivided cell. Symmetric ketones could be obtained from good to excellent yields by applying mild

electrochemical conditions. In light of the analyzed data by combination of reactivity, cyclic voltammetry, spectroelectrochemistry, and DFT calculations, we suggest a sophisticated synergistic effect between the two catalysts **FeTTPCI** and **1Ni**. Both catalysts are instrumental in achieving the ketones with high yield. However, when **FeTTPCI** is alone results in the formation of toluene and carboxylation products. This fact illustrates that **FeTTPCI**, besides facilitating the reduction of CO<sub>2</sub>-to-CO, also promotes the BnCl to Bn<sup>-</sup> anion formation. Then, the carbonylation most likely happens at the nickel coordination sphere, although some of the Bn<sup>-</sup> may also be derived from the **FeTTP** catalytic activity. As such, the exact mechanism underpinning these processes is more challenging than initially hypothesized, as both catalysts might serve dual roles. Nevertheless, based on thermodynamic considerations, the substitution of the chloride anion with benzyl anion in the intermediate [Ni(bpy)(Bn)(CO)Cl] (−23.0 kcal·mol<sup>-1</sup>, considering a [Bn<sup>-</sup>] of 1·10<sup>-6</sup> M) present as a more plausible mechanism than potential Ni disproportionation reactions (−6.2 kcal·mol<sup>-1</sup>).

The results open a further dimension of cooperative interaction between electrocatalysts, emphasizing the complexity of electrocatalytic reactions and the need for further mechanistic investigations, which are ongoing in our laboratory. We expect these results will encourage others to explore and capitalize on potential synergies in electrocatalysis. Finally, using CO<sub>2</sub> as a CO surrogate can simplify experimental setups, reduce the use of toxic CO, and facilitate the production of labeled compounds.

## Acknowledgements

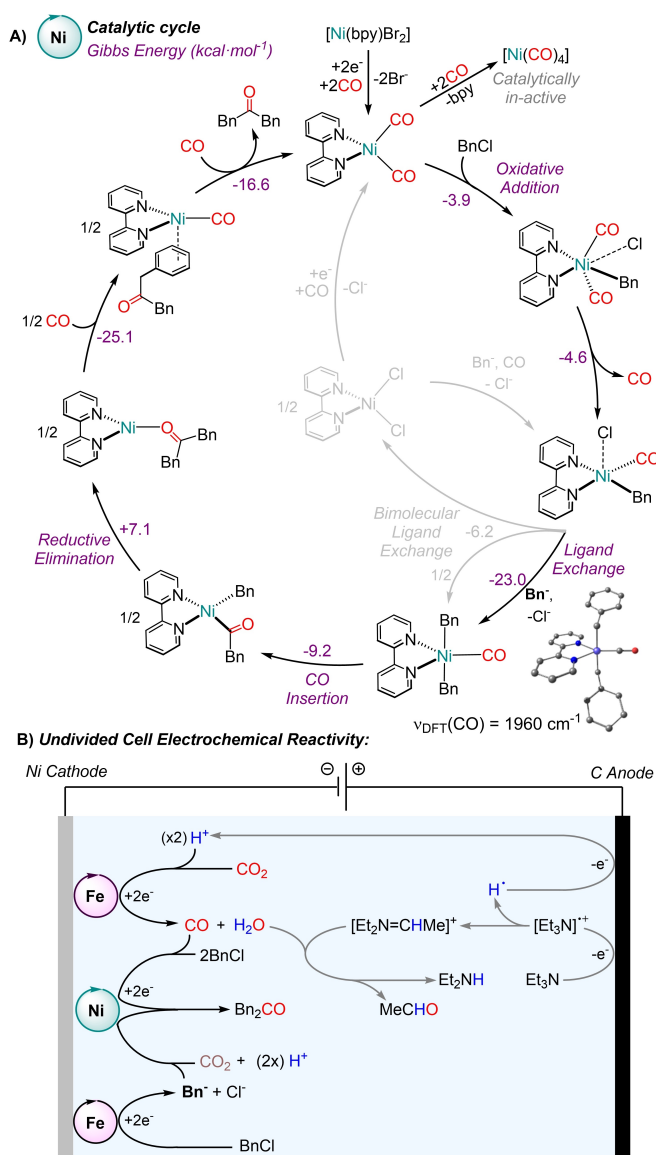
The authors acknowledge the financial support of the ICIQ Foundation, the CERCA Program/Generalitat de Catalunya, MICINN through Severo Ochoa Excellence Accreditation 2020–2023 (CEX2019-000925-S, MIC/AEI), the European Research Foundation for H2020 project ERC-2015-CoG GREENLIGHT\_REDCAT 648304, (J.L.-F.), the Spanish Ministry of Universities for an FPU fellowship FPU16/04234 (S.F.), AGAUR (2021-SGR-01260, J.L.-F.) and MICINN (PID2019-110050RB-I00, J.L.-F., PID2022-140142OB-I00, TED2021-132790B-I00, PDC2022-133451-I00). C.L. and A.S. MICINN-PFI Scholarship for a predoctoral fellowship (PID2019-110050RB-I00).

## Conflict of Interest

The authors declare no conflict of interest.

## Data Availability Statement

The data that support the findings of this study are available from the corresponding author upon reasonable request.



**Scheme 3.** Proposed reaction mechanism for the Ni/Fe-catalyzed benzyl chloride carbonylation.

**Keywords:** Electrocatalysis · CO<sub>2</sub> valorization · cascade reaction · carbonylation · dual catalysis

- [1] a) A. A. Kelkar, in *Industrial Catalytic Processes for Fine and Specialty Chemicals* (Eds.: S. S. Joshi, V. V. Ranade), Elsevier, Amsterdam **2016**, pp. 663–692; b) J.-B. Peng, H.-Q. Geng, X.-F. Wu, *Chem* **2019**, *5*, 526–552; c) M. R. Didgikar, S. S. Joshi, in *Industrial Catalytic Processes for Fine and Specialty Chemicals* (Eds.: S. S. Joshi, V. V. Ranade), Elsevier, Amsterdam **2016**, pp. 693–719; d) Q. Tian, X. Yin, R. Sun, X. F. Wu, Y. Li, *Coord. Chem. Rev.* **2023**, *475*, 214900; e) J.-B. Peng, F.-P. Wu, X.-F. Wu, *Chem. Rev.* **2019**, *119*, 2090–2127.
- [2] a) B. Zhang, W. Deng, Z.-Y. Xu, *Organometallics* **2023**, *42*, 588–596; b) X. Liu, T. An, Z. Yin, W. Zhang, *Chem. Eur. J.* **2023**, *29*, e202202880.
- [3] a) J. Chen, S. Zhu, *J. Am. Chem. Soc.* **2021**, *143*, 14089–14096; b) H. Chen, H. Yue, C. Zhu, M. Rueping, *Angew. Chem. Int. Ed.* **2022**, *61*, e202204144; c) A. Rérat, C. Michon, F. Agbossou-Niedercorn, C. Gosmini, *Eur. J. Org. Chem.* **2016**, *2016*, 4554–4560; d) R. Shi, X. Hu, *Angew. Chem. Int. Ed.* **2019**, *58*, 7454–7458.
- [4] a) B. Panda, G. Albano, *Catalysts* **2021**, *11*, 1531; b) Y. Wan, M. Alterman, M. Larhed, A. Hallberg, *J. Org. Chem.* **2002**, *67*, 6232–6235; c) D. Nageswar Rao, S. Rasheed, P. Das, *Org. Lett.* **2016**, *18*, 3142–3145; d) Y.-Z. Chen, T.-H. Ding, Q.-Q. Li, J.-P. Qu, Y.-B. Kang, *Org. Lett.* **2023**, *25*, 2611–2615.
- [5] a) F. Xu, D. Li, W. Han, *Green Chem.* **2019**, *21*, 2911–2915; b) G. Sun, M. Lei, L. Hu, *RSC Adv.* **2016**, *6*, 28442–28446; c) P. Sharma, S. Rohilla, N. Jain, *J. Org. Chem.* **2017**, *82*, 1105–1113; d) Z. Li, L. Wang, *Adv. Synth. Catal.* **2015**, *357*, 3469–3473; e) F. A. Sofi, G. Dubey, R. Sharma, P. Das, P. V. Bharatam, *Tetrahedron* **2020**, *76*, 131060; f) P. Kannaboina, G. Raina, K. Anil Kumar, P. Das, *Chem. Commun.* **2017**, *53*, 9446–9449; g) S. N. Gockel, K. L. Hull, *Org. Lett.* **2015**, *17*, 3236–3239; h) G. K. Rathod, R. Jain, *J. Org. Chem.* **2023**.
- [6] a) S. Fu, S. Yao, S. Guo, G.-C. Guo, W. Yuan, T.-B. Lu, Z.-M. Zhang, *J. Am. Chem. Soc.* **2021**, *143*, 20792–20801; b) X. He, Y. Cao, X.-D. Lang, N. Wang, L.-N. He, *ChemSusChem* **2018**, *11*, 3382–3387; c) W. Xiong, B. Wu, B. Zhu, X. Tan, L. Wang, W. Wu, C. Qi, H. Jiang, *ChemCatChem* **2021**, *13*, 2843–2851.
- [7] a) D. U. Nielsen, X.-M. Hu, K. Daasbjerg, T. Skrydstrup, *Nat. Catal.* **2018**, *1*, 244–254; b) R. Sang, Y. Hu, R. Razaq, G. Mollaert, H. Atia, U. Bentrup, M. Sharif, H. Neumann, H. Junge, R. Jackstell, B. U. W. Maes, M. Beller, *Nat. Commun.* **2022**, *13*, 4432.
- [8] a) L. Zeng, H. Li, S. Tang, X. Gao, Y. Deng, G. Zhang, C.-W. Pao, J.-L. Chen, J.-F. Lee, A. Lei, *ACS Catal.* **2018**, *8*, 5448–5453; b) Y. Wu, L. Zeng, H. Li, Y. Cao, J. Hu, M. Xu, R. Shi, H. Yi, A. Lei, *J. Am. Chem. Soc.* **2021**, *143*, 12460–12466; c) C. Xu, *Chin. J. Org. Chem.* **2020**, *40*, 2600–2602; d) L. Zeng, H. Li, J. Hu, D. Zhang, J. Hu, P. Peng, S. Wang, R. Shi, J. Peng, C.-W. Pao, J.-L. Chen, J.-F. Lee, H. Zhang, Y.-H. Chen, A. Lei, *Nat. Catal.* **2020**, *3*, 438–445; e) S. C. Sau, R. Mei, J. Struwe, L. Ackermann, *ChemSusChem* **2019**, *12*, 3023–3027; f) J. Zhang, B. Das, O. Verho, J.-E. Bäckvall, *Angew. Chem. Int. Ed.* **2022**, *61*, e202212131; g) S. Xie, Y. Yin, Y. Wang, J. Wang, X. He, R. Bai, R. Shi, *Green Chem.* **2023**, *25*, 1522–1529; h) I. Chiarotto, M. Feroci, *Tetrahedron Lett.* **2001**, *42*, 3451–3453.
- [9] a) F. Franco, C. Rettenmaier, H. S. Jeon, B. Roldan Cuenya, *Chem. Soc. Rev.* **2020**, *49*, 6884–6946; b) F. Franco, M. F. Pinto, B. Royo, J. Lloret-Fillol, *Angew. Chem. Int. Ed.* **2018**, *57*, 4603–4606; c) S. Fernández, F. Franco, C. Casadevall, V. Martín-Diaconescu, J. M. Luis, J. Lloret-Fillol, *J. Am. Chem. Soc.* **2020**, *142*, 120–133; d) M. Claros, F. Ungeheuer, F. Franco, V. Martín-Diaconescu, A. Casitas, J. Lloret-Fillol, *Angew. Chem. Int. Ed.* **2019**, *58*, 4869–4874.
- [10] a) C. Costentin, G. Passard, M. Robert, J.-M. Savéant, *Proc. Natl. Acad. Sci. USA* **2014**, *111*, 14990–14994; b) C. Costentin, S. Drouet, M. Robert, J.-M. Savéant, *Science* **2012**, *338*, 90–94; c) M. Hammouche, D. Lexa, J. M. Savéant, M. Mointeau, *J. Electroanal. Chem. Interfacial Electrochem.* **1988**, *249*, 347–351.
- [11] a) W. Zhang, L.-L. Liao, L. Li, Y. Liu, L.-F. Dai, G.-Q. Sun, C.-K. Ran, J.-H. Ye, Y. Lan, D.-G. Yu, *Angew. Chem. Int. Ed.* **2023**, *n/a*, e202301892; b) L. Li, N. Fu, *Chem* **2023**, *9*, 556–558; c) M. Surke, R. Zhao, L. Ackermann, *Sci. China Chem.* **2023**; d) G.-Q. Sun, P. Yu, W. Zhang, W. Zhang, Y. Wang, L.-L. Liao, Z. Zhang, L. Li, Z. Lu, D.-G. Yu, S. Lin, *Nature* **2023**, *615*, 67–72; e) Z. Zhao, Y. Liu, S. Wang, S. Tang, D. Ma, Z. Zhu, C. Guo, Y. Qiu, *Angew. Chem. Int. Ed.* **2023**, *62*, e202214710; f) K. Zhang, B.-H. Ren, X.-F. Liu, L.-L. Wang, M. Zhang, W.-M. Ren, X.-B. Lu, W.-Z. Zhang, *Angew. Chem. Int. Ed.* **2022**, *61*, e202207660; g) Y. Wang, S. Tang, G. Yang, S. Wang, D. Ma, Y. Qiu, *Angew. Chem. Int. Ed.* **2022**, *61*, e202207746; h) Y. You, W. Kanna, H. Takano, H. Hayashi, S. Maeda, T. Mita, *J. Am. Chem. Soc.* **2022**, *144*, 3685–3695; i) L.-L. Liao, Z.-H. Wang, K.-G. Cao, G.-Q. Sun, W. Zhang, C.-K. Ran, Y. Li, L. Chen, G.-M. Cao, D.-G. Yu, *J. Am. Chem. Soc.* **2022**, *144*, 2062–2068; j) G.-Q. Sun, W. Zhang, L.-L. Liao, L. Li, Z.-H. Nie, J.-G. Wu, Z. Zhang, D.-G. Yu, *Nat. Commun.* **2021**, *12*, 7086; k) X.-T. Gao, Z. Zhang, X. Wang, J.-S. Tian, S.-L. Xie, F. Zhou, J. Zhou, *Chem. Sci.* **2020**, *11*, 10414–10420; l) W. Zhang, S. Lin, *J. Am. Chem. Soc.* **2020**, *142*, 20661–20670; m) N. W. J. Ang, J. C. A. Oliveira, L. Ackermann, *Angew. Chem. Int. Ed.* **2020**, *59*, 12842–12847; n) Y. Kim, G. D. Park, M. Balamurugan, J. Seo, B. K. Min, K. T. Nam, *Adv. Sci.* **2020**, *7*, 1900137; o) A. M. Sheta, A. Alkayal, M. A. Mashaly, S. B. Said, S. S. Elmorsy, A. V. Malkov, B. R. Buckley, *Angew. Chem. Int. Ed.* **2021**, *60*, 21832–21837; p) A. M. Sheta, M. A. Mashaly, S. B. Said, S. S. Elmorsy, A. V. Malkov, B. R. Buckley, *Chem. Sci.* **2020**, *11*, 9109–9114; q) A. Alkayal, V. Tabas, S. Montanaro, I. A. Wright, A. V. Malkov, B. R. Buckley, *J. Am. Chem. Soc.* **2020**, *142*, 1780–1785; r) D.-T. Yang, M. Zhu, Z. J. Schiffer, K. Williams, X. Song, X. Liu, K. Manthiram, *ACS Catal.* **2019**, *9*, 4699–4705; s) K.-J. Jiao, Z.-M. Li, X.-T. Xu, L.-P. Zhang, Y.-Q. Li, K. Zhang, T.-S. Mei, *Org. Chem. Front.* **2018**, *5*, 2244–2248.
- [12] L. Garnier, Y. Rollin, J. Périchon, *J. Organomet. Chem.* **1989**, *367*, 347–358.
- [13] M. Oçafraïn, M. Devaud, M. Troupel, J. Périchon, *J. Chem. Soc. Chem. Commun.* **1995**, 2331–2332.
- [14] a) E. Dolhem, R. Barhdadi, J. C. Folest, J. Y. Nédélec, M. Troupel, *Tetrahedron* **2001**, *57*, 525–529; b) E. Dolhem, M. Oçafraïn, J. Y. Nédélec, M. Troupel, *Tetrahedron* **1997**, *53*, 17089–17096.
- [15] M. T. Jensen, M. H. Rønne, A. K. Ravn, R. W. Juhl, D. U. Nielsen, X.-M. Hu, S. U. Pedersen, K. Daasbjerg, T. Skrydstrup, *Nat. Commun.* **2017**, *8*, 489.
- [16] a) R. Miró, E. Fernández-Llamazares, C. Godard, M. Díaz de los Bernardos, A. Gual, *Chem. Commun.* **2022**, 10552–10555; b) P. Gotico, A. Del Vecchio, D. Audisio, A. Quaranta, Z. Halime, W. Leibl, A. Aukauloo, *ChemPhotoChem* **2018**, *2*, 715–719.
- [17] a) L. Ponsard, E. Nicolas, N. H. Tran, S. Lamaison, D. Wakerley, T. Cantat, M. Fontecave, *ChemSusChem* **2021**, *14*, 2198–2204; b) H. M. Dodge, B. S. Natinsky, B. J. Jolly, H. Zhang, Y. Mu, S. M. Chapp, T. V. Tran, P. L. Diaconescu, L. H. Do, D. Wang, C. Liu, A. J. M. Miller, *ACS Catal.* **2023**, *13*, 4053–4059.
- [18] J. C. Siu, N. Fu, S. Lin, *Acc. Chem. Res.* **2020**, *53*, 547–560.
- [19] a) D. Lexa, J. Mispelter, J. M. Saveant, *J. Am. Chem. Soc.* **1981**, *103*, 6806–6812; b) D. Lexa, J. M. Saveant, D. L. Wang, *Organometallics* **1986**, *5*, 1428–1434; c) D. G. Boucher, Z. A. Nguyen, S. D. Minter, *Faraday Discuss.* **2023**.

- [20] R. J. Perkins, D. J. Pedro, E. C. Hansen, *Org. Lett.* **2017**, *19*, 3755–3758.
- [21] I. Bhugun, D. Lexa, J.-M. Saveant, *J. Am. Chem. Soc.* **1994**, *116*, 5015–5016.
- [22] a) C. P. Andrieux, I. Gallardo, J. M. Savaent, K. B. Su, *J. Am. Chem. Soc.* **1986**, *108*, 638–647; b) C. Gueutin, D. Lexa, J. M. Saveant, D. L. Wang, *Organometallics* **2002**, *8*, 1607–1613; c) D. Lexa, J. M. Saveant, B. Su Khac, D. L. Wang, *J. Am. Chem. Soc.* **1989**, *110*, 7617–7625; d) P. J. Brothers, *Adv. Organomet. Chem.* **2000**, *44*, 223–321.
- [23] W. Liu, M. N. Lavagnino, C. A. Gould, J. Alcázar, D. W. C. MacMillan, *Science* **2021**, *374*, 1258–1263.
- [24] C. P. Andrieux, C. Blocman, J. M. Dumas-Bouchiat, F. M'Halla, J. M. Savéant, *J. Electroanal. Chem. Interfacial Electrochem.* **1980**, *113*, 19–40.
- [25] R. S. Wade, C. E. Castro, *J. Am. Chem. Soc.* **1973**, *95*, 226–230.
- [26] a) I. M. Arafa, K. Shin, H. M. Goff, *J. Am. Chem. Soc.* **2002**, *110*, 5228–5229; b) C. Gueutin, D. Lexa, M. Momenteau, J. M. Saveant, *J. Am. Chem. Soc.* **1990**, *112*, 1874–1880.
- [27] a) A. B. Dürr, H. C. Fisher, I. Kalvet, K.-N. Truong, F. Schoenebeck, *Angew. Chem. Int. Ed.* **2017**, *56*, 13431–13435; b) I. Kalvet, Q. Guo, G. J. Tizzard, F. Schoenebeck, *ACS Catal.* **2017**, *7*, 2126–2132; c) M. I. Lipschutz, T. D. Tilley, *Angew. Chem. Int. Ed.* **2014**, *53*, 7290–7294; d) T. Tang, A. Hazra, D. S. Min, W. L. Williams, E. Jones, A. G. Doyle, M. S. Sigman, *J. Am. Chem. Soc.* **2023**, *145*, 8689–8699; e) C. Amatore, A. Jutand, J. Périchon, Y. Rollin, *Monatsh. Chem.* **2000**, *131*, 1293–1304.
- [28] P. A. Christensen, A. Hamnett, S. J. Higgins, J. A. Timney, *J. Electroanal. Chem.* **1995**, *395*, 195–209.
- [29] K. Teiji, K. Sanshiro, Y. Takakazu, Y. Akio, *Chem. Lett.* **1979**, *8*, 1513–1516.
- [30] J. K. Beattie, T. W. Hambley, A. F. Masters, J. T. Meyer, *Inorg. Chim. Acta* **1993**, *213*, 49–55.

Manuscript received: February 23, 2024

Version of record online: April 22, 2024